metals

MDPI

Article

Case Study to Illustrate the Potential of Conformal Cooling Channels for Hot Stamping Dies Manufactured Using Hybrid Process of Laser Metal Deposition (LMD) and Milling

Magdalena Cortina [1,*], Jon Iñaki Arrizubieta [1], Amaia Calleja [1], Eneko Ukar [1] and Amaia Alberdi [2]

[1] Department of Mechanical Engineering, University of the Basque Country, Plaza Torres Quevedo 1, 48013 Bilbao, Spain; joninaki.arrizubieta@ehu.eus (J.I.A.); amaia.calleja@ehu.eus (A.C.); eneko.ukar@ehu.eus (E.U.)

[2] Tecnalia Research and Innovation—Industrial Systems Unit, Paseo Mikeletegi 7, 20009 Donostia/San Sebastián, Spain; amaia.alberdi@tecnalia.com

* Correspondence: magdalena.cortina@ehu.eus; Tel.: +34-946-017-347

Received: 12 December 2017; Accepted: 30 January 2018; Published: 1 February 2018

Abstract: Hot stamping dies include cooling channels to treat the formed sheet. The optimum cooling channels of dies and molds should adapt to the shape and surface of the dies, so that a homogeneous temperature distribution and cooling are guaranteed. Nevertheless, cooling ducts are conventionally manufactured by deep drilling, attaining straight channels unable to follow the geometry of the tool. Laser Metal Deposition (LMD) is an additive manufacturing technique capable of fabricating nearly free-form integrated cooling channels and therefore shape the so-called conformal cooling. The present work investigates the design and manufacturing of conformal cooling ducts, which are additively built up on hot work steel and then milled in order to attain the final part. Their mechanical performance and heat transfer capability has been evaluated, both experimentally and by means of thermal simulation. Finally, conformal cooling conduits are evaluated and compared to traditional straight channels. The results show that LMD is a proper technology for the generation of cooling ducts, opening the possibility to produce new geometries on dies and molds and, therefore, new products.

Keywords: additive manufacturing; laser metal deposition; hot stamping; die and mold; conformal cooling; design optimization

1. Introduction

The die and mold industry plays a significant role in the manufacturing world [1]. This is due to the fact that nearly all mass-produced parts are manufactured employing processes that include dies and molds, directly affecting not only the efficiency of the process, but also the quality of the product [2]. Moreover, increasing demand in the automotive industry for high strength and lightweight components has led to the promotion and development of hot stamping (also known as Press Hardening) processes [3]. Through this technique, a boron steel blank is heated until austenization at temperatures between 900 °C and 950 °C inside a furnace and then transferred to an internally cooled die set, where it is simultaneously stamped and quenched. The transformation of austenite into martensite occurs thanks to a rapid cooling of the blank, at a temperature range of 420–280 °C, along which the dies must be actively cooled at a minimum cooling rate of 27 °C·s^{-1} [4]. The temperature of the hot stamping tool must be kept below 200 °C in order to ensure the cooling of the blank, achieve high strength and prolong the lifespan of the tools [5]. Thus, if the cooling ducts are

not adequately designed, the temperature of the tool can be increased during the productive process, the quenching may not be successfully achieved and therefore, the final product would not meet requirements. Moreover, the temperature of the die could be non-homogeneous, resulting in hot areas where the quenching could not be achieved.

The efficiency of the cooling channels determines the characteristics and cooling time of the final part. Some authors [6] relate low cooling rates and thermally induced surface defects on the component to an inadequate cooling system. These consequences could be avoided by the optimization and new arrangement of the cooling ducts. However, the cooling conduits are conventionally manufactured by drilling, hence only straight channels can be generated and often attain a not uniform heat transfer. This may lead to longer cycle times, unequal cooling and warp [7]. Thus, the employment of traditional techniques for the manufacture of the inner cooling conducts of the stamping tools leads to restrictions on the final geometry of the parts.

Additive manufacturing technologies such as LMD have been developed within recent years, enabling the manufacture of high quality and fully dense metal parts. Reducing porosity is one of the main objectives in order to achieve good quality and mechanical properties in additively manufactured components. Some authors [8,9] perform meticulous studies in order to determine the effect of main process parameters on the metallurgy of the parts. Additive Manufacturing offer a real solution when manufacturing conformal cooling channels with complex geometries and, therefore, advance towards rapid cooling [10].

There are two kinds of techniques for manufacturing conformal cooling ducts in hot stamping molds or dies: the layer-laminated method and the powder metallurgy-based additive manufacturing, belonging powder bed and powder nozzle technologies to the latter [11]. On the one hand, by layer-laminated manufacturing, single layers are cut, stacked and then joined together in order to generate a final part. This technique is used for the production of plain and geometrically simple parts. For instance, Hölker et al. [12] studied the design of straight holes in layered extrusion dies by joining lamellas with holes and thus creating cooling channels. On the other hand, components are additively built up layer by layer by locally melting a metal powder bed or stream, implying freeform manufacturing with nearly no geometric restrictions. These methods are usually performed to generate high complexity geometries and, regarding LMD, it is frequently combined with machining, giving rise to the so-called hybrid manufacturing.

Huskic et al. [13,14] investigated the integration of conformal cooling channels into forging dies and hot stamping tools by using Selective Laser Melting (SLM). Results showed that the hybrid die could withstand the mechanical loads originated during forging. In addition, Ahn et al. [15] manufactured injection molds with conformal cooling ducts by combining direct metal rapid tooling and machining. As a result, the designed molds highly reduced the cooling time and required energy when compared to the conventional molds, improving the product quality. Müller et al. [16] manufactured hybrid hot stamping dies by machining and additively building up inserts with conformal cooling ducts. As a result, the additively manufactured channels cooled six times faster than the conventional drilled channels. With regard to powder nozzle-based additive technologies, Vollmer et al. [17] studied the integration and manufacturing of additively built up cooling channels for the fabrication of hot stamping tools. For this purpose, several grooves were machined and afterwards closed by LMD and finished by milling. From the literature review, it is noted that some research has been carried out in the field of conformal cooling and additive manufacturing. However, the number of references focusing on the application and suitability of these technologies to hot stamping tools is very limited. Hence, there exists a gap in the generation of conformal channels by depositing hot work steels, such as AISI H13 on CR7V-L, and the analysis of the resultant thermal and mechanical characteristics.

The present work aims to investigate the design and manufacturing of additively built up conformal cooling ducts, fabricated by combining LMD with 5-axis milling. Experimental study of laser metal deposition of AISI H13 tool steel powder on CR7V-L tool steel specimens has been carried out for the fabrication of the adaptive cooling channels. The performance of the channels is

analyzed and compared to traditional straight ducts by metallurgical, mechanical tests and thermal analysis. Finally, the suitability of this process to a 3D geometry of higher complexity is investigated.

2. Materials and Methods

All experiments described in this work are performed on a 5-axis (three linear and two rotatory) conventional milling center rebuilt as a laser processing machine, named Kondia Aktinos 500 (Kondia, Elgoibar, Spain), whose work piece size capacity is 700 × 360 × 380 mm^3. In addition, a high power Yb:YAG fiber laser source, Rofin FL010 (ROFIN-SINAR Laser GmbH, Bergkirchen, Germany), is used, with a maximum power output of 1 kW, emitting wavelength of 1070 nm and pulse frequency range up to 5 kHz. The laser beam is guided through an optical multi-mode fiber from the laser source to the processing machine, generating a circular laser spot of 2 mm on the surface of the work piece, situated at a 200 mm focal distance. The powder is fed by means of a Sulzer Metco Twin 10-C powder feeder (Oerlikon Metco, Pfäffikon, Switzerland) and an in-house designed coaxial nozzle, EHU/Coax 2015 (UPV/EHU, Bilbao, Spain) [18], while argon is used as both drag and shielding gas.

Three different materials are used along the present investigation in order to generate the final part: CR7V-L, AISI H13 (1.2344) (Flame Spray Technologies, Duiven, The Netherlands) and AISI 316L (1.4404) (Erasteel, Commentry, France). On the one hand, CR7V-L hot work tool steel by Kind and Co. Edelstahlwerk, Wiehl, Germany [19] is a special high Cr-alloyed steel commonly used in hot work applications, such as hot forming tools of structural automobile parts. Furthermore, it is characterized by excellent high temperature strength and wear resistance, as well as good thermal fatigue resistance. On the other hand, AISI H13 is a Cr-Mo-V alloyed tool steel with a high level of resistance to thermal shock and fatigue and good temperature strength. Thus, these properties make AISI H13 particularly valuable for tooling. The chemical composition and thermal properties of the studied materials are shown in Tables 1 and 2, respectively.

Table 1. Chemical composition (wt. %) of the used materials, data from [19–22].

Material	C	Si	Mn	Cr	Mo	V	Ni	P	Fe
CR7V-L	0.42	0.50	0.40	6.50	1.30	0.80	-	-	Balance
AISI H13	0.39	1.00	0.40	5.20	1.40	0.90	-	-	Balance
AISI 316L	0.0023	0.34	0.079	18.15	2.33	-	11.75	<0.001	Balance

Table 2. Thermal properties of the used materials, data from [19–22].

Material	Temperature (°C)	20	400	600
CR7V-L	Thermal conductivity ($W{\cdot}m^{-1}{\cdot}K^{-1}$)	26.7	30.8	30.8
	Coefficient of thermal expansion (10^{-6} K^{-1})	11.2	12.5	13.1
AISI H13	Thermal conductivity ($W{\cdot}m^{-1}{\cdot}K^{-1}$)	25	29	30
	Coefficient of thermal expansion (10^{-6} K^{-1})	-	12.6	13.2
AISI 316L	Thermal conductivity ($W{\cdot}m^{-1}{\cdot}K^{-1}$)	15.3	20.1	22.7
	Coefficient of thermal expansion (10^{-6} K^{-1})	16	17.5	18.5

Hence, CR7V-L slabs are used as substrate and AISI H13 metallic powder as filler material so that the conformal cooling channels are closed. Both materials are compatible hot work tool steels with similar thermal properties, such as thermal conductivity and coefficient of thermal expansion. Besides, AISI 316L austenitic stainless steel is used as intermediate layer in order to relax internal stress and improve the weldability of the materials. Otherwise, the direct deposition of AISI H13 with no intermediate layer results in the cracking of the part. The preference of choosing AISI 316L instead of other interface materials such as nickel alloys is due to its higher thermal conductivity and ease of LMD.

The present investigation is performed on a 100 × 120 × 32 mm^3 CR7V-L hot work steel slab, in which two different cooling channels of six millimeters of diameter at a depth of ten millimeters

below the surface are generated: one is conventionally drilled and the other additively manufactured via LMD, see Figure 1. At first, the CR7V-L substrate is soft annealed by holding the specimen at 840 °C for five hours with slow cooling in furnace (Helmut ROHDE GmbH, Prutting, Germany) in order to reduce its high hardness, 59.6 HRC, and allow its preparation by machining. This preparation consists of directly drilling a first duct and milling a 45° V-notch for the LMD operation. Once the preparatory phase is concluded, the part is ready to be submitted to the LMD process, whose aim is to close the milled V-notch so that an additively manufactured channel comparable to the drilled one is generated. Moreover, accessibility issues and geometric restrictions are considered for verifying the suitability of the available nozzle when manufacturing the part.

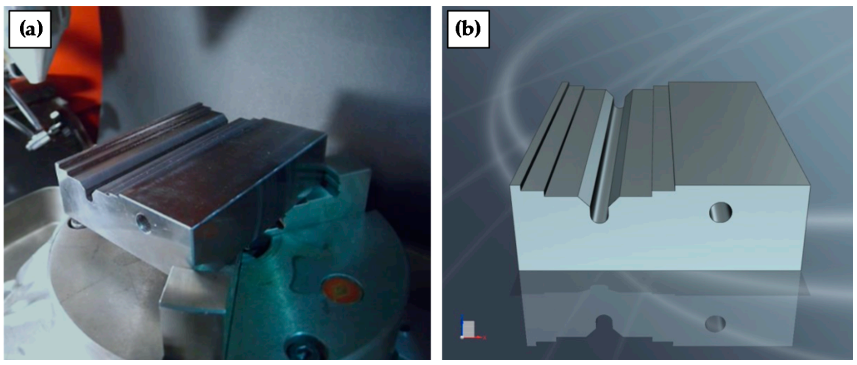

Figure 1. (**a**) Substrate before LMD; (**b**) Computer Aided Design (CAD) model to be processed.

Along the LMD process, two different materials are deposited: AISI 316L stainless steel as intermediate layer and AISI H13 hot work steel for the surface coating. Different deposition strategies and process parameters are used for attaining sound clads with each material. Firstly, AISI 316L is used in order to seal the V-notch and hence generate the channel, while AISI H13 is added over it until the upper surface of the part is reached. For that purpose, the AISI 316L intermediate layer is deposited on the right and left slopes of the milled V-notch alternately, following a longitudinal zigzag cladding strategy in which the surface of the part and the nozzle are perpendicularly orientated as shown in Figure 2.

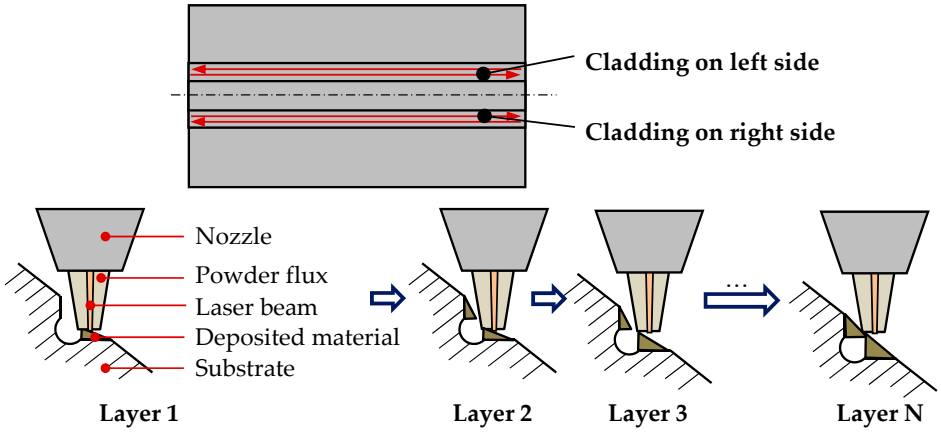

Figure 2. Deposition strategy of the AISI 316L intermediate layer.

Once the channel is closed, AISI H13 is added by alternating longitudinal with transversal directions when laser cladding until the desired height is reached, as shown in Figure 3. Directionality within the mechanical properties and residual stress of the deposited material that may lead to the generation of cracks are thereby avoided.

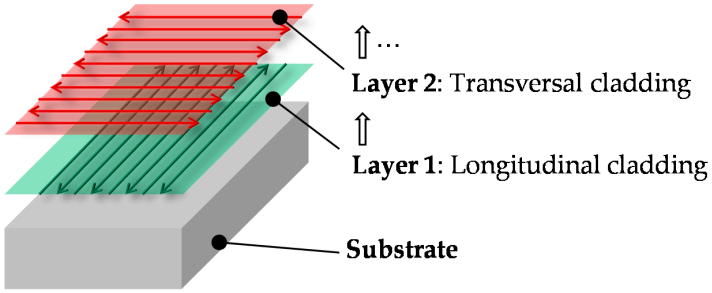

Figure 3. Deposition strategy of AISI H13.

As far as the process parameters are concerned, different values are used for the deposition of each material and are presented in Table 3, while the results attained when finishing the deposition of AISI 316L and AISI H13 are shown in Figure 4.

Table 3. Laser Metal Deposition (LMD) process parameters regarding deposited materials.

Process Parameters	AISI 316L	AISI H13
Continuous wave (CW) laser power (W)	625	600
Scan velocity (mm·min^{-1})	550	450
Track offset (mm)	1.4	1
Overlap (%)	30	50
Powder flow rate (g·min^{-1})	5	3.3
Powder preheating temperature (°C)	60	
Protective gas flow rate (L·min^{-1})	14	

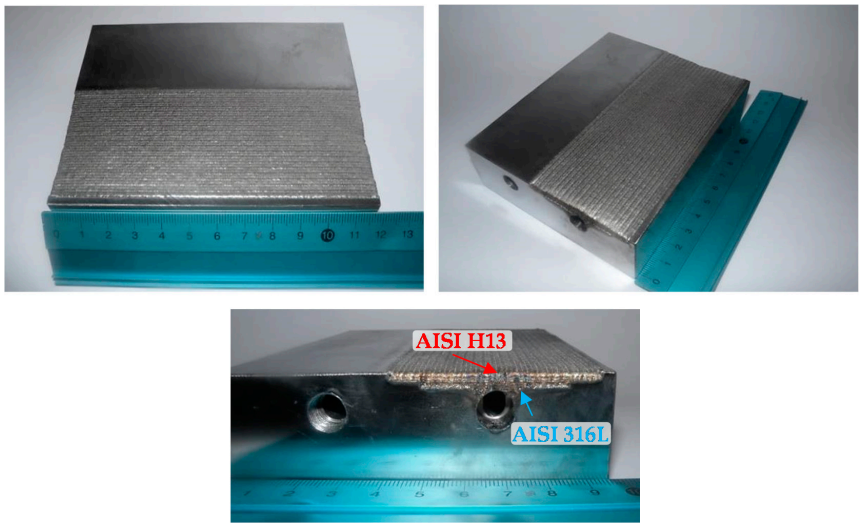

Figure 4. Final part after finishing the LMD process.

Following the experiments, the part is hardened by heating at 1050 °C for 15 min and quenching in water. The component is then ground so that the desired surface quality is attained. In addition, drill holes of ten millimeters length are conducted and M10 fine threaded inside the channels in order to enable the threading of push in connectors and then proceed to the thermal and mechanical analyses.

3. Results

3.1. Analysis of Microstructure and Internal Defects

In order to analyze the macrostructure and microstructure of the deposited material and find possible internal defects, the cross section of samples was cut, polished and etched. Marble solution was used to reveal macrostructure and microstructure of the substrate and deposited material. Images of cross sections are offered, where the macrostructure properties of the clads are shown. The strategy of deposition of the different layers can be appreciated in Figure 5a, where the deposition directions are indicated.

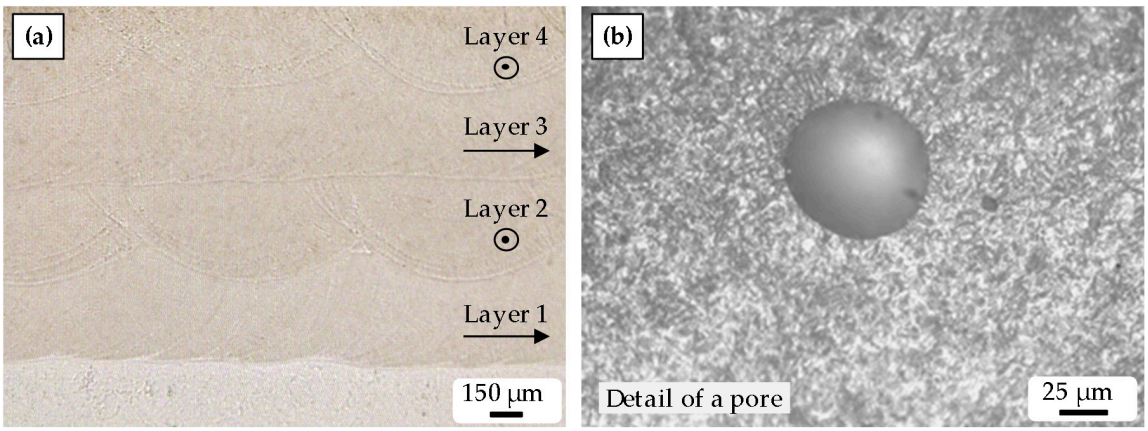

Figure 5. Metallography of the (**a**) deposited layers; (**b**) detail of a pore.

As far as metallurgical quality is concerned, no cracks or other intra- or inter-layer defects are detected, except for some intra-layer pores of less of 100 μm diameter. An example is shown in Figure 5b, where a higher magnification of an intra-layer region is shown and a pore of approximately 75 μm diameter can be noted.

Furthermore, a detail of the microstructures of substrate and clad is shown in Figure 6. The substrate (Figure 6a) presents a martensitic microstructure characteristic of tempered CR7V-L. From Figure 6b, it may be noted that the morphology of the microstructure of the deposited AISI H13 is principally martensitic, composed of retained austenite and some undissolved carbides distributed in a tempered martensite matrix.

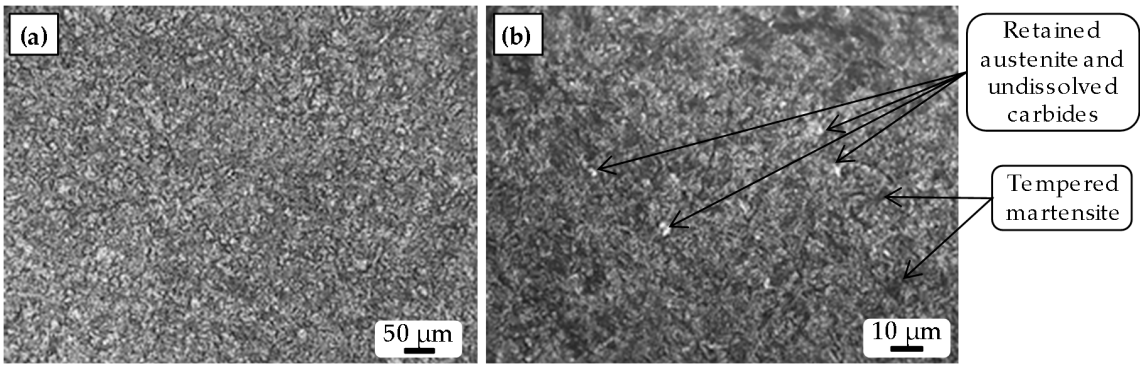

Figure 6. Microstructure of (**a**) the substrate; (**b**) the deposited material.

Hence, the analysis of the microstructure and the quality of the deposited material result to be satisfactory and no anomalies are found.

3.2. Thermal Analysis

3.2.1. Cooling Capacity

In order to analyze the cooling capacity of the drilled and additively built up channels, the specimen is monitored with an Optris PI 160 infrared camera (Optris Infrared Sensing, Portsmouth, NH, USA), while the emissivity of the material is evaluated with a type K thermocouple. For that purpose, the sample is heated by scanning the surface with the laser at 1000 W. The scanner sweeps a rectangular area and its thermal evolution is examined both with active and inactive water-cooling. Three points are monitored: one for each channel (LMD manufactured and drilled) and a third one for the center of the part, while a water flow of 1 $L \cdot min^{-1}$ is inserted through the connectors previously threaded.

On the one hand, the cooling capacity when the laser and the cooling are active is studied. Along this test, the laser and the cooling work simultaneously and maximum temperatures of around 60 °C are reached. Both ducts cool the part down equally so that the part does not heat up; however, the temperature regarding the LMD channel is slightly higher, as it can be appreciated in Figure 7.

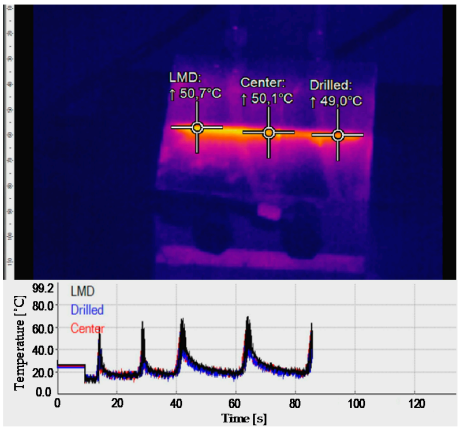

Figure 7. Cooling capacity when laser and water-cooling are both active.

On the other hand, the cooling capacity after a temperature of 100 °C is reached is analyzed. In this case, the water-cooling remains inactive until a temperature value of 100 °C is accomplished. The water-cooling is then activated, with the subsequent temperature descent and cooling down of the part. The temperatures obtained for both channels share once again similar values, with a maximum difference of 5 °C and being slightly higher on the LMD duct, as shown in Figure 8.

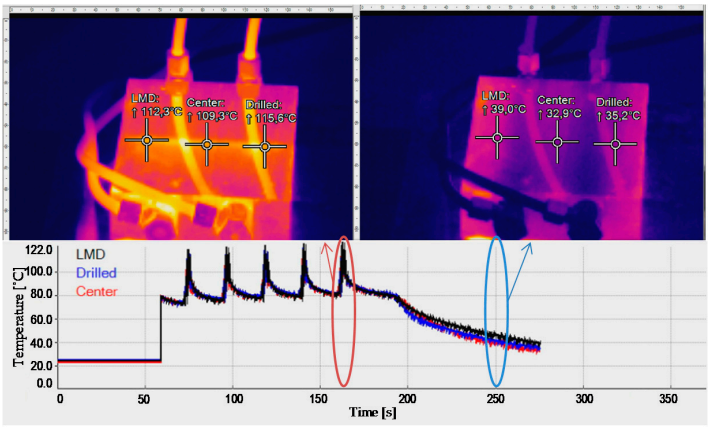

Figure 8. Cooling capacity when the water-cooling is active after reaching 100 °C.

By comparing the cooling capacity of the LMD manufactured and drilled channels on both tests performed, it is concluded that both ducts work similarly during the heating and cooling cycles with a very slight difference on their temperature values. This difference can be due to the existence of the AISI 316L stainless steel intermediate layer, whose thermal conductivity is noticeably lower than the ones regarding AISI H13 and CR7V-L tool steels. The thermal effect of the stainless steel intermediate layer is therefore analyzed by means of thermal simulations.

3.2.2. Thermal Simulations

The selected LMD strategy includes the deposition of a stainless steel intermediate layer, whose thermal properties differ from the ones of the original part. Moreover, the surface finish of the LMD channel is coarser than the one regarding the drilled duct. Hence, the influence of the intermediate layer and the surface finish is studied by means of finite elements (FE) thermal simulations, where the effect of both issues on the thermal conductivity and cooling process of the part are analyzed.

On the one hand, the results of the thermal simulations for both drilled and LMD cooling channels along a 120 s period are shown and compared to real results in Figure 9. A good correspondence is attained, as the relative error committed is below 5%, what involves a high reliability of the simulations.

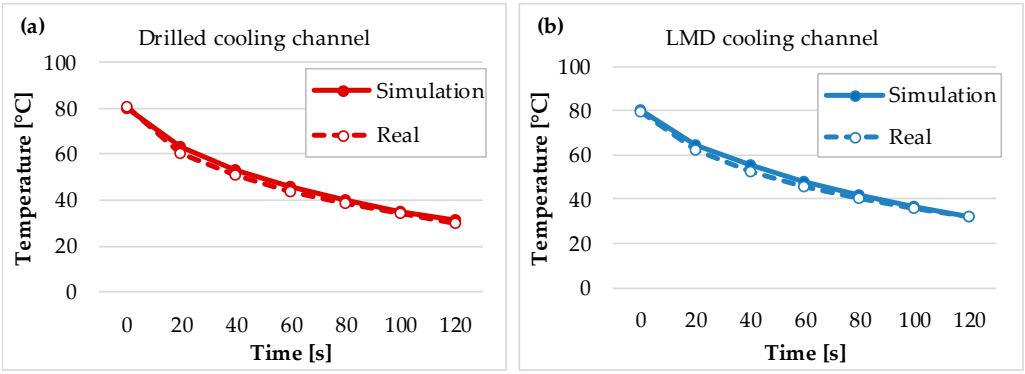

Figure 9. Simulation and real results for (**a**) drilled; (**b**) LMD cooling channels.

On the other hand, a comparison between the evolutions of the temperatures of both ducts is shown in Figure 10. Therefore and according to the simulations, it can be concluded that both channels work similarly and the effect of surface finish together with the influence of the stainless steel intermediate layer is negligible.

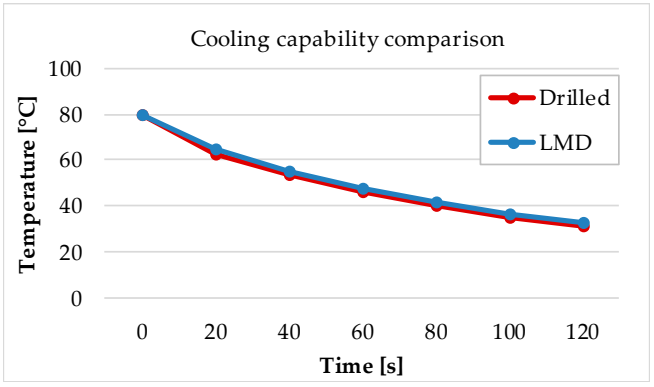

Figure 10. Cooling capacity comparison between the drilled and the LMD channels.

Hence, the simulations are satisfactory and the two ducts experience the same cooling. The temperature of the part is reduced from 80 °C until 30 °C in 120 s for both channels.

3.3. Mechanical Analysis

3.3.1. Compression Test

Once the cooling capacity of the additively built up channel of the manufactured part is positively compared to the drilled duct, a mechanical validation of the specimen is accomplished. The service conditions of a die are limited to a maximum pressure of 12–15 MPa at a velocity of 50–80 mm·s^{-1}. However, and because of the restrictions of the available compression machine, the tests are realized at a velocity of 40 mm·min^{-1}. The technical characteristics of the employed machine are included in Table 4.

Table 4. Technical characteristics of the compressive machine.

Technical Characteristics of the SDE Compressive Machine (MEM-101/SDC)	
Capacity (kN)	300
Maximum velocity (mm·min^{-1})	40
Stroke (mm)	400

Two different experiments are carried out attending to the pressure applied. On the first compression test, CT1, the force is applied on the whole surface of the specimen, while on the second compression test, CT2, the pressure is localized on the channels. For that purpose, two ten millimeters width AISI 1020 rectangular bars are placed over the channels. For each compression test, two different pressures are applied: one according to the maximum pressure on service, 15 MPa, and another with a safety factor of two when possible, resulting in a pressure value of 30 MPa. Regarding the CT1-2 test, it is not possible to reach 30 MPa because of exceeding the maximum force of 300 kN to be applied by the compressive machine, 25 MPa are therefore applied. The parameters of the compression tests performed are shown in Table 5.

Table 5. Realized compression tests.

Test	Applied Pressure (MPa)	Surface (mm^2)	Applied Force (kN)
CT1-1	15	11,677.5	175.16
CT1-2	25	11,677.5	291.94
CT2-1	15	2404	36.06
CT2-2	30	2404	72.12

The evolution of the applied force regarding the stroke of the machine on the most critical executed tests is shown in the following charts hereunder shown in Figure 11. At first, the value of the force is zero because of the existing gap between the upper compressor plate and the part. Then, a minimum value of force is reached, after which a linear increasing tendency of the force with regard to the stroke of the upper plate is appreciated.

The part is visually analyzed after the realization of the mechanical tests and no changes are detected. Possible cracking and deformation are inspected by means of penetrating liquids and a dial gauge, respectively. Results show that no distortions or cracks are present in the deposited area. Thus, it is concluded that the additively built up channel withstands the service pressure of 15 MPa, even with a safety factor of two. The manufactured specimen subsequently meets the mechanical requirements necessary in hot stamping dies.

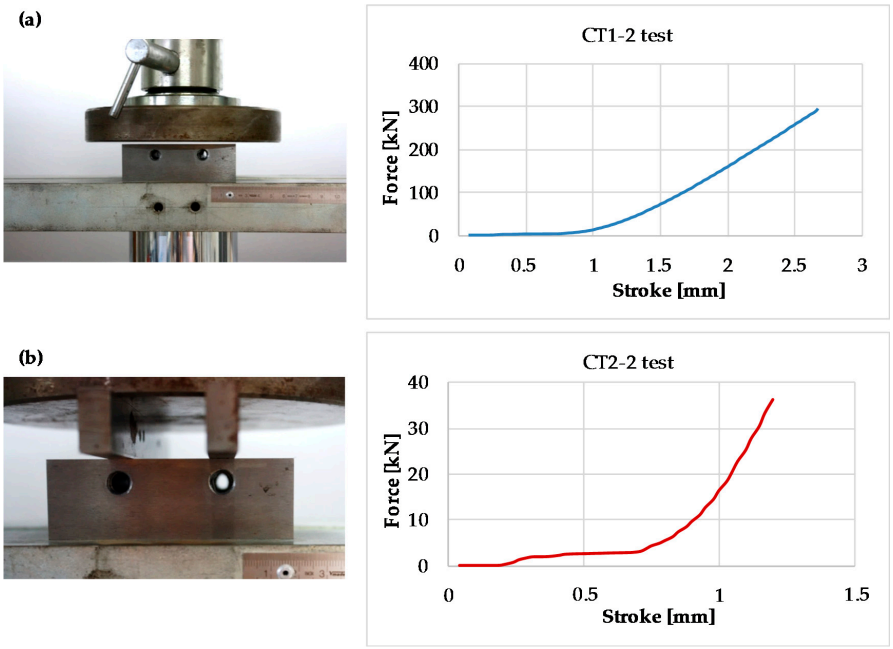

Figure 11. (**a**) CT1-2; (**b**) CT2-2 set-ups and results.

3.3.2. Hardness and Roughness Tests

Additionally, with regard to the compression tests, hardness is measured both superficially and across the different layers deposited. Surface measurements were realized at 49 N (5 kgf) with an Ernst Compumet SC hardness tester (ERNST Härteprüfer SA, Lamone, Switzerland), obtaining an average hardness of 55.45 HRC, which is higher than the 50 HRC value required by the specification of the tool. The hardness measurements along the cross section were performed at 2.9 N (0.3 kgf) using a micro-Vickers hardness tester, Future-Tech FM-800 (Future-Tech Corp., Kawasaki, Japan), and the dwell time was 12 s. The Vickers hardness values across the different layers of material are shown in Figure 12.

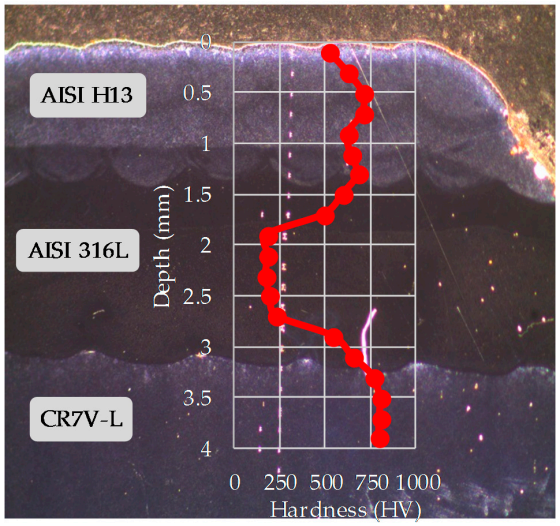

Figure 12. Vickers hardness values of the deposited materials and substrate.

On the one hand, the AISI H13 upper layer generally presents similar hardness values than the CR7V-L substrate. However, the superficial area of the AISI H13 layer presents a slightly lower hardness

of 523.8 HV. On the other hand, as it was expected, the hardness of the intermediate AISI 316L layer is considerably lower. This is due to the mechanical properties of the material itself, whose maximal hardness value is of 200 HV [23], approximately. With regard to roughness, mean roughness, Ra, is measured along the cladding direction with a profilometer, Taylor Hobson Form Talysurf Series 2 (Taylor Hobson, Leicester, UK), obtaining a Ra value of 3.11 µm. The hardness and roughness values of the final part are therefore satisfactory according to the materials and technology employed.

3.4. 3D Conformal Cooling

After verifying the use of LMD for generating suitable conformal cooling channels on hot stamping tools, the ability of the process with regard to more complex geometries is studied. For that purpose, the following geometrical challenge shown in Figure 13 is proposed, where the cooling duct is perfectly adapted to the shape of the part.

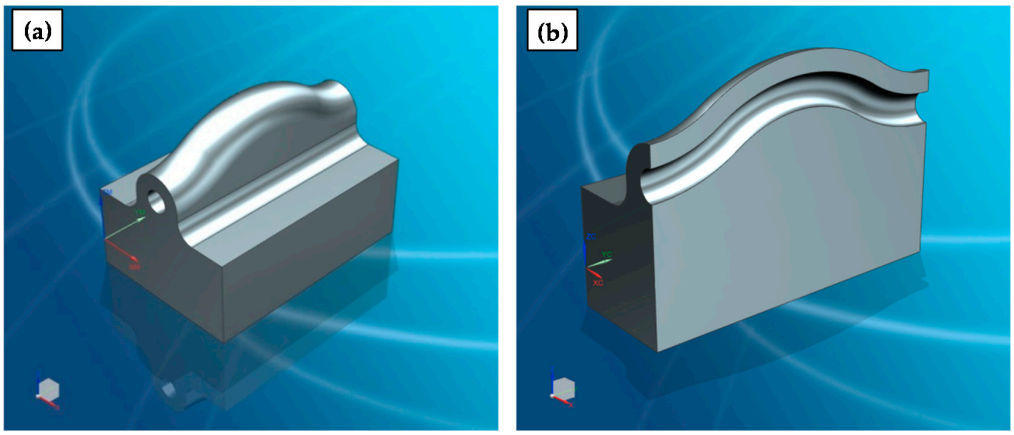

Figure 13. (**a**) Isometric view; (**b**) cross section of the 3D conformal cooling CAD model.

The experimental procedure and methodology followed in this case is analogous to those previously detailed in Section 2. Materials and Methods. The 100 × 70 × 70 mm^3 CR7V-L substrate is firstly soft annealed so that the machining preliminary to the LMD process is eased, attaining a hardness of 30–35 HRC, see Figure 14.

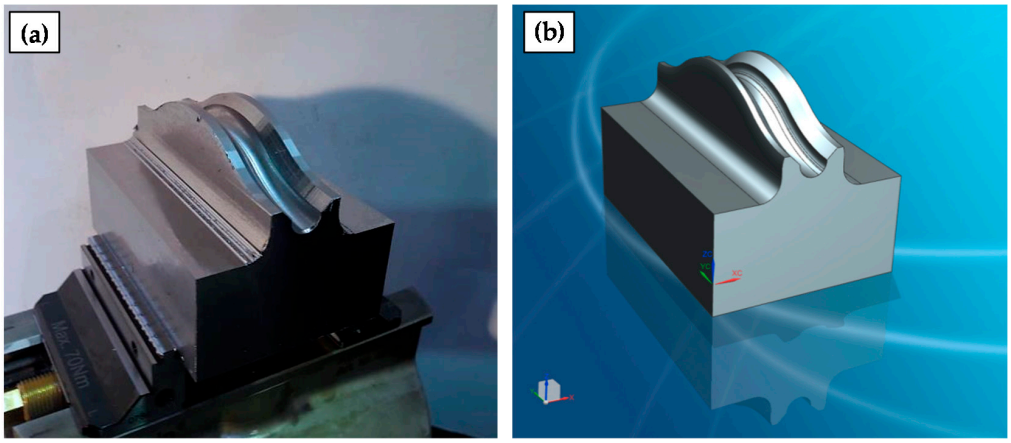

Figure 14. (**a**) Substrate before LMD; (**b**) CAD model after the preparatory machining.

Once the preparatory milling stage is concluded, the additive closure of the cooling duct is conducted by the 5-axis deposition of AISI 316L and AISI H13. In this case, a suitable building strategy is developed for the execution of the LMD process by using the CAD model (NX 11, Siemens Industry

Software Ltd., Frimley, Surrey, UK, 2017) data to generate the deposition paths. First of all, AISI 316L is used for V-notch sealing (Figure 15a). The material is added following a triangle geometry so that the material added in one side of the conduct does not interfere with the material added on the other side and the conduct is perfectly closed. Afterwards, AISI H13 is added until the upper surface of the desired geometry is reached. These last strategies have been programmed with NX11 from Siemens®. Zig/Zag strategy is followed in the added layers alternatively (Figure 15c,d).

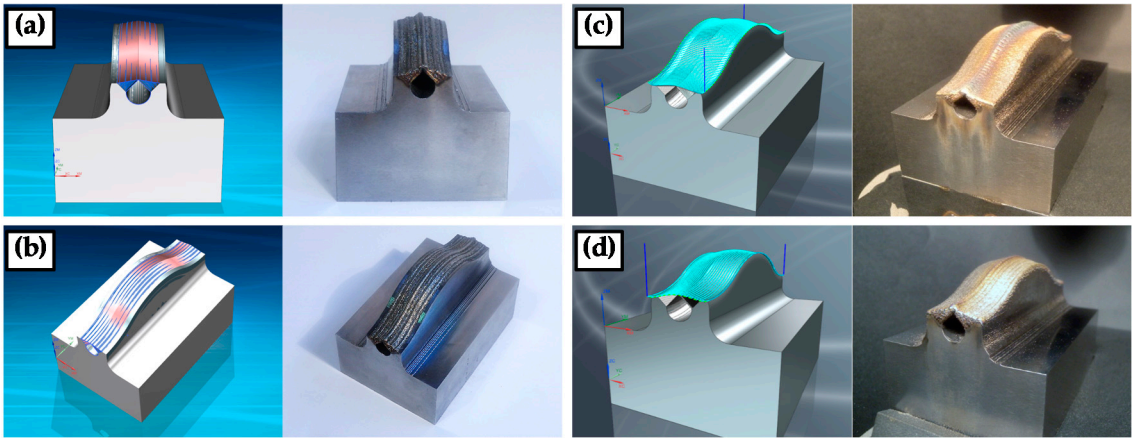

Figure 15. (**a**) Front; (**b**) lateral views of the resulting part after LMD; (**c**) transversal LMD; (**d**) longitudinal LMD.

In order to obtain a "near-to-net-shape" geometry, the layers width is reduced for upper layers gradually. This way, a semi-cylinder geometry is created and machining times are reduced because of a lower volume of material to be machined. The resulting near-net-shape part is shown in Figure 16.

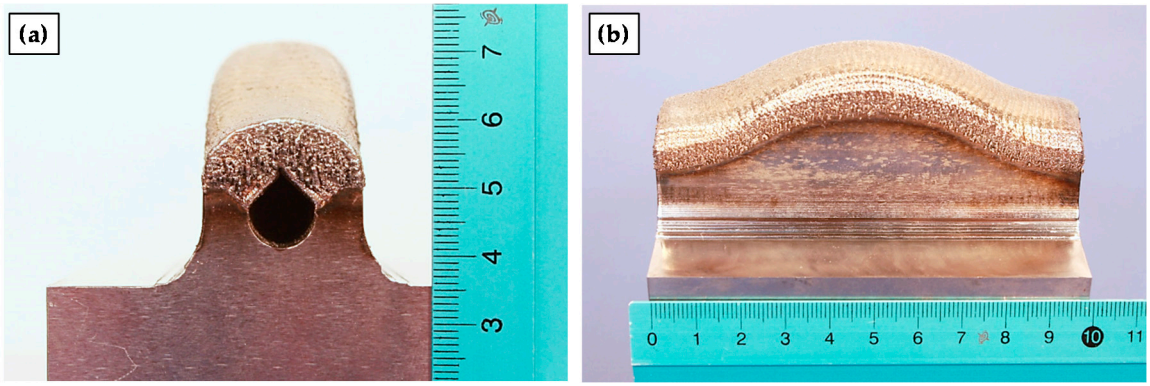

Figure 16. (**a**) Front; (**b**) lateral views of the resulting part after LMD.

Because of the LMD process, residual stresses are generated. Annealing the specimen so that the residual stresses are relieved is strongly recommended. The annealing process is a conventional treatment that consists of keeping the sample at 650 °C for a holding time of two hours, slow cooling to 500 °C and free cooling in air. The part is consequently milled and hardened before the last finishing milling operation, aiming to attain a higher hardness when finished. The hardening consists of heating the part at 1050 °C for 15 min and then quenching in water.

The final specimen is then subjected to a non-destructive test via X-ray radiography, X-Cube compact 225 (General Electric, Boston, MA, USA), in order to verify its internal structure and integrity. The results are shown in Figure 17b, where the geometry of the internal cooling channel is also appreciated.

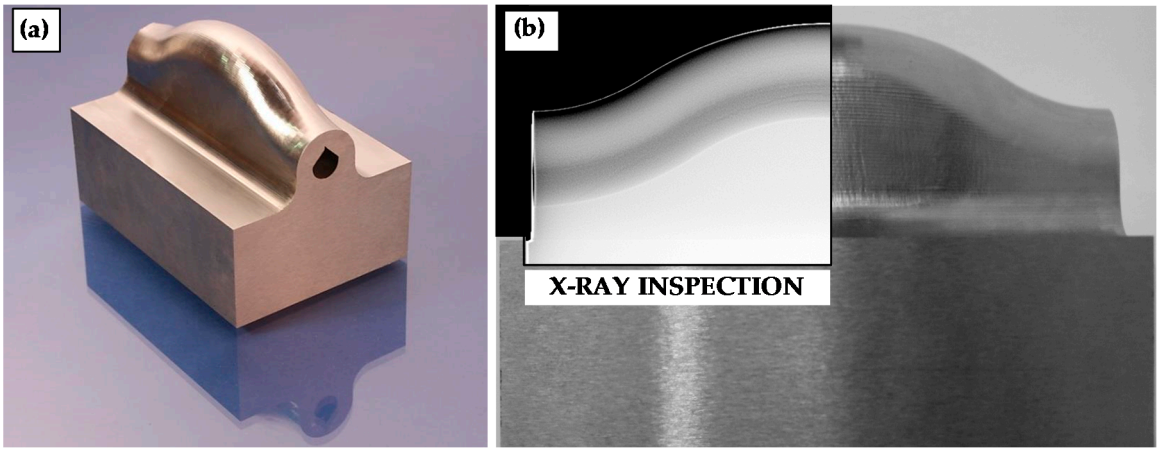

Figure 17. (**a**) Final part; (**b**) X-ray inspection.

3.5. Conformal Cooling via Thermal Simulations

With the aim of demonstrating the thermal benefits of conformal cooling, a comparison between the new adaptive channel and the conventionally straight channel is realized by means of thermal simulations. An analysis of the performance of both types of cooling ducts is shown in Figure 18, where the hot stamping of a sheet metal blank is simulated.

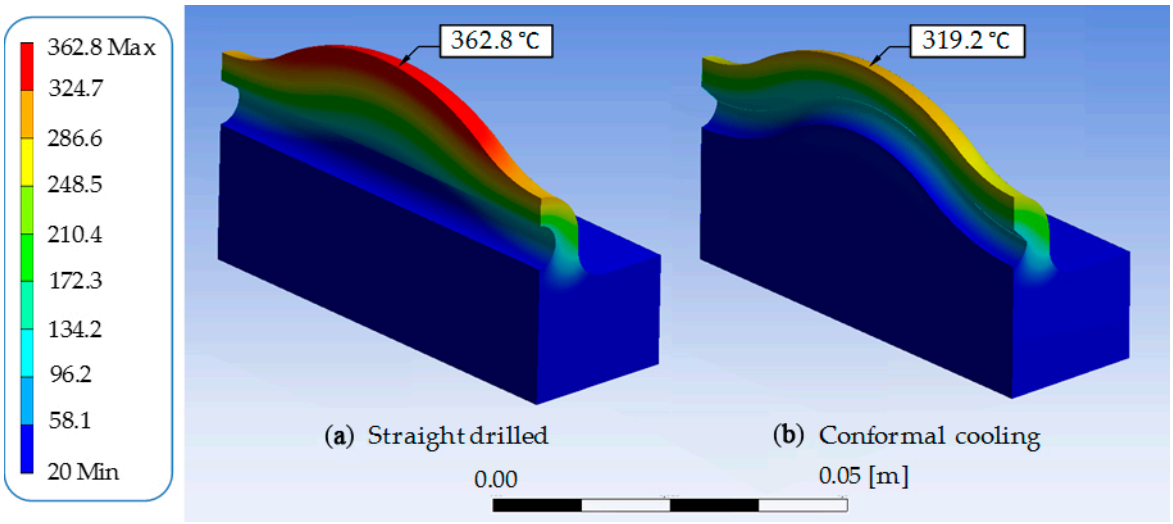

Figure 18. Thermal simulation results of conventional drilled (**a**) vs. conformal (**b**) cooling.

At the initial time step and according to the process, the bulk temperature is of 20 °C and the heated metal sheet is at 900 °C. Temperature distributions after 5 s are displayed.

As expected, the temperature distribution of the conformal part is more homogeneous than in the drilled specimen, following the geometry of the channel. Moreover, at the same time instant, lower temperatures are reached. This may imply a higher cooling rate of the conformal channel. Therefore, additively built up cooling channels present the same performance as drilled channels, when they have the very same geometry. However, the main benefit of conformal channels is the possibility of adapting to more complex cooling system designs and their constant distance to the die surface.

4. Discussion

In the present work, the design and manufacturing of conformal cooling ducts via additive manufacturing is investigated. Their mechanical performance and heat transfer capability are evaluated, both experimentally and by thermal simulations. According to the obtained results, the following conclusions can be drawn:

(1) In general terms, it can be concluded that the strategy of generating cooling channels via LMD is a viable alternative to traditional techniques regarding the metallurgical quality and mechanical and thermal characteristics achieved on the manufactured die. Previous experiments performed with this approach demonstrate the attainability of minimum channel diameters of down to 3 mm and minimum wall thicknesses of 2 mm.

(2) With regard to thermal characteristics, a more homogeneous temperature distribution within the tool and the stamped part is attained, leading to the enhancement of the dimensional accuracy and features of the produced parts. Moreover, the betterment of the temperature distribution also leads to the lowering of the process cycle times in hot stamping and the subsequent improvement of the efficiency of the process and reduction of the costs.

(3) Apart from meeting the mechanical requirements demanded by the hot stamping process, the built-up channel is smooth and without projected material, leading to a good internal quality. In addition, the lack of pre and post heating cycles during the LMD process together with the absence of inserts for the generation of the channel ease the process as far as industrialization issues are concerned.

Hence, this work demonstrated the capability of achieving good mechanical and thermal properties for additively manufactured conformal cooling hot stamping dies. Therefore, the advances in LMD processes open doors for new designs, which may enable the generation of more complex geometries and hence innovate towards the manufacturing of new parts.

Acknowledgments: This study was supported by the H2020-FoF13 PARADDISE Project (Grant Agreement No. 723440) and the ADDICLEAN Project (RTC-2015-4194-5) of the Spanish Ministry of Economy and Competitiveness and the University of the Basque Country (UPV/EHU). Special thanks are addressed to Batz S. Coop. Company (Igorre, Spain) for their technical support in this work.

Author Contributions: Jon Iñaki Arrizubieta and Magdalena Cortina conceived and designed the experiments; Jon Iñaki Arrizubieta, Magdalena Cortina and Amaia Calleja performed the experiments; Jon Iñaki Arrizubieta realized the thermal simulations and Magdalena Cortina analyzed the data; Eneko Ukar and Amaia Alberdi contributed materials/analysis tools; Magdalena Cortina wrote the paper.

Conflicts of Interest: The authors declare no conflict of interest.

References

1. Jhavar, S.; Paul, C.P.; Jain, N.K. Causes of failure and repairing options for dies and molds: A review. *Eng. Fail. Anal.* **2013**, *34*, 519–535. [CrossRef]
2. Altan, T.; Lilly, B.; Yen, Y.C.; Altan, T. Manufacturing of Dies and Molds. *CIRP Ann.* **2001**, *50*, 404–422. [CrossRef]
3. Steinbeiss, H.; So, H.; Micheltisch, T.; Hoffmann, H. Method for Optimizing the Cooling Design of Hot Stamping Tools. *Prod. Eng.* **2007**, *1*, 149–155. [CrossRef]
4. Eriksson, M.; Oldenburg, M.; Somani, M.C.; Karjalainen, L.P. Testing and Evaluation of Material Data for Analysis of Dorming and Hardening of Boron Steel Components. *Model. Simul. Mater. Sci. Eng.* **2002**, *10*, 277–294. [CrossRef]
5. Hoffmann, H.; So, H.; Steinbeiss, H. Design of hot stamping tools with cooling system. *CIRP Ann.* **2007**, *56*, 269–272. [CrossRef]
6. Hölker, R.; Jäger, A.; Tekkaya, A.E. Additive manufacturing of tools and dies for metal forming. In *Laser Additive Manufacturing*; Brandt, M., Ed.; Woodhead Publishing Series in Electronic and Optical Materials; Woodhead Publishing: Cambridge, UK, 2017; Volume 17, pp. 439–464.

7. Shinde, M.S.; Ashtankar, K.M. Additive manufacturing-assisted conformal cooling channels in mold manufacturing processes. *Adv. Mech. Eng.* **2017**, *9*, 1–14. [CrossRef]
8. Campanelli, S.L.; Angelastro, A.; Signorile, C.G.; Casalino, G. Investigation on direct laser powder deposition of 18 Ni (300) marage steel using mathematical model and experimental characterization. *Int. J. Adv. Manuf. Technol.* **2017**, *89*, 885–895. [CrossRef]
9. Casalino, G.; Campanelli, S.L.; Contuzzi, N.; Ludovico, A.D. Experimental investigation and statistical optimisation of the selective laser melting process of a maraging steel. *Opt. Laser Technol.* **2015**, *65*, 151–158. [CrossRef]
10. Schieck, F.; Hochmuth, C.; Polster, S.; Mosel, A. Modern tool design for component grading incorporating simulation models, efficient tool cooling concepts and tool coating systems. *CIRP J. Manuf. Sci. Technol.* **2011**, *4*, 189–199. [CrossRef]
11. Hölker, R.; Haase, M.; Khalifa, N.B.; Tekkaya, A.E. Hot extrusion dies with conformal cooling channels produced by Additive Manufacturing. *Mater. Today Proc.* **2015**, *2*, 4838–4846. [CrossRef]
12. Hölker, R.; Jäger, A.; Khalifa, N.B.; Tekkaya, A.E. New concepts for cooling of extrusion dies manufactured by rapid tooling. *Key Eng. Mater.* **2011**, *491*, 223–232. [CrossRef]
13. Huskic, A.; Behrens, B.A.; Giedenbacher, J.; Huskic, A. Standzeituntersuchungen generative hergestellter Schmiedewerkzeuge. *Schmiede J.* **2013**, *92013*, 66–70.
14. Huskic, A.; Giedenbacher, J.; Pschebezin, U.; Wild, N. Rapid Tooling für Umformwerkzeuge. *RTejournal Forum für Rapid Technologie* **2012**.
15. Ahn, D.G.; Kim, H.W.; Park, S.H. Manufacture of mould with a high energy efficiency using rapid manufacturing process. *AIP Conf. Proc.* **2010**, *1252*, 185–191.
16. Müller, B. *Konturnahe Temperierung beim Presshärten*; Fraunhofer Institut für Werkzeugmaschinen und Umformtechnik (IWU): Chemnitz, Germany, 2013.
17. Vollmer, R.; Kolleck, R.; Schwemberger, P. Herstellung oberflächennaher kühlkanalstrukturen für das presshärten mittels Laserauftragschweißen. In Proceedings of the Tagungsband zum 9. Erlanger Workshop Warmblechumformung, Erlangen, Germany, 18 November 2014; pp. 61–73.
18. Arrizubieta, J.I.; Tabernero, I.; Ruiz, J.E.; Lamikiz, A.; Martínez, S.; Ukar, E. Continuous coaxial nozzle design for LMD based on numerical simulation. *Phys. Procedia* **2014**, *56*, 429–438. [CrossRef]
19. Kind & Co Edelstahlwerk. CR7V-L Datasheet. Available online: http://www.kind-co.de/en/download-centre.html (accessed on 17 September 2017).
20. Uddeholm. Orvar Supreme Datasheet. Available online: http://www.uddeholm.com/files/PB_orvar_supreme_english.pdf (accessed on 17 September 2017).
21. Metallied Powder Solutions SA. *Pearl® Micro 316L Datasheet*; Metallied Powder Solutions SA: San Sebastian, Spain, 2015.
22. AK Steel Corporation. 316/316L Stainless Steel Datasheet. Available online: http://www.aksteel.com/pdf/markets_products/stainless/austenitic/316_316l_data_sheet.pdf (accessed on 28 September 2017).
23. Sandmeyer Steel Company. Specification Sheet: Alloy 316/316L. Available online: https://www.sandmeyersteel.com/images/316-316l-317l-spec-sheet.pdf (accessed on 28 September 2017).